Desalination and Water Treatment
www.deswater.com

doi: 10.1080/19443994.2013.836999

53 (2015) 158–170
January

Taylor & Francis
Taylor & Francis Group

Adsorption performance of APTMS-DTPA/PVDF chelating membrane toward Ni(II) with the presence of Ca(II), NH_4^+, lactic acid, and citric acid

Laizhou Song*, Mo Yang, Jie Fu, Pingping Lu, Xiuli Wang, Jun He

College of Environmental and Chemical Engineering, Yanshan University, Qinhuangdao 066004, China
Tel. +86 3358387741; Fax: +86 3358061569; email: songlz@ysu.edu.cn

Received 16 April 2013; Accepted 5 August 2013

ABSTRACT

The 3-aminopropyltrimethoxysilane-diethylenetriaminepentaacetic acid/polyvinylidene fluoride (APTMS-DTPA/PVDF) chelating membrane was prepared to remove Ni(II) from the solutions. The adsorption performance of the membrane toward Ni(II) was investigated by the adsorption experiments and density functional theory (DFT) calculations, considering the existence of Ca(II), NH_4^+, lactic acid, and citric acid. Ca(II) tended to form more stable complex with the APTMS-DTPA ligand of the chelating membrane than NH_4^+. Citric acid showed a larger interference on Ni(II) uptake than lactic acid. Lagergren second-order equation and Langmuir model were competent for descriptions of the adsorption kinetics and the isotherms, respectively. The negative ΔG° and ΔH° indicated the spontaneous and exothermic nature of Ni(II) adsorption. The results of DFT calculations were consistent with the experimental data. The complexing sequences of the metal ions with the APTMS-DTPA ligand were in the order of NH_4^+ < Ca(II) < Ni(II). The stabilities of the Ni(II)–organic complexes followed the order of Ni(II)–lactic acid < Ni(II)–citric acid < Ni(II)–(APTMS-DTPA). Therefore, the complexation between Ni(II) and APTMS-DTPA ligand of the membrane was prominent.

Keywords: Chelating membrane; Adsorption; Coexistent cation; Nickel–organic complex; Density functional theory

1. Introduction

Nickel ion identified as a carcinogen has shown the significantly toxic influences on human beings and ecological systems [1,2]. The inhalation of nickel and its compounds can lead to lung diseases and malignant tumors. In China, nickel electroless plating and electroplating industries discharge a large amount of wastewater, which has posed a threat to the ecosystem. Emission of wastewater containing Ni(II) has been controlled strictly, and the discharged concentration of total nickel should not exceed 0.1 mg/l according to the published "Emission standard of pollutants for electroplating" (GB 21,900-2008, China). Therefore, wastewater containing nickel should be treated to maintain the legislative standard. In the effluents of the binary nickel electroless plating processes, the cations involving Ca(II) and NH_4^+, and the organic acid reagents containing lactic acid and citric acid always coexist with Ni(II). The aforementioned cations and organic acids will hinder the removal of Ni(II) [3], thereby, the development of effective techniques to inactivate and recover Ni(II)

*Corresponding author.

with the presence of the coexistent cations and organic acids, is thus of great importance.

Compared with the traditional methods used to remove Ni(II) from solutions including chemical coagulation and precipitation, ion exchange and adsorption, solvent extraction, biosorption and electrocoagulation, the membrane separation techniques have become increasingly attractive for the disposal of Ni(II), due to the advantages of time-saving, lower pressure drop and shorter axial-diffusion path [4,5]. However, in comparison with the conventional exchange resin adsorption process, the membrane techniques applied to remove Ni(II) involving electrodialysis [6], liquid membrane extraction [7], polymer-enhanced filtration [8,9], nanofiltration, and reverse osmosis [10,11] have been restricted to a certain extent because of the higher costs or the more fussy pretreatments.

The complexing adsorption of the chelating membrane has been a very efficient way to inactivate and remove heavy metals [12]. In our previous research [13], it has been confirmed that melamine-diethylenetriaminepentaacetic acid/polyvinylidene fluoride (MA-DTPA/PVDF) chelating membrane can recover Ni(II) with the presence of the coexistent cations and organic acids. This kind of PVDF-based chelating membrane can perform the function of recovering Ni(II) from the spent nickel electroless plating bath. However, the above-mentioned chelating membrane will be not suitable for the practical application due to the low adsorption capacity. The improvement of adsorption performance for the PVDF-based chelating membrane bearing DTPA complexing group, thus deserves to be considered.

As an important supplement of the experimental methods, the density functional theory (DFT) simulation has been used to study various chemical problems well [14,15]. The DFT descriptors, including chemical potential (μ), hardness (η), electrophilicity index (ω) and condensed Fukui function (FF), have been confirmed efficiently to define and justify the concepts of chemical reactivity [16–18]. To our knowledge, however, insufficient attention has been devoted to the adsorption of aqueous metals by means of DFT simulation mentioned above.

In this research, another kind of PVDF-based chelating membrane with a characteristic of higher Ni(II) uptake than the previous MA-DTPA/PVDF chelating membrane, namely 3-aminopropyltrimethoxysilane-diethylenetriaminepentaacetic acid/polyvinylidene fluoride (APTMS-DTPA/PVDF) chelating membrane was prepared to recover Ni(II) from the simulated wastewater. The batch adsorption experiments of APTMS-DTPA/PVDF chelating membrane toward Ni(II) were performed regarding the presence of the cations, including Ca(II) and NH_4^+, and the organic acids involving lactic acid and citric acid. The thermodynamic and kinetic adsorption characteristics of the chelating membrane with the presence of the cations and organic acids mentioned above were also analyzed. To further understand the influences of the aforementioned cations and organic acids on the chelating membrane toward Ni(II), the global DFT descriptors including μ, η, and ω were calculated to explore the chemical reactivity of the APTMS-DTPA complexing ligand of the membrane, Ni(II), Ca(II), NH_4^+, lactic acid, and citric acid. The condensed FF (f_k^+ for electrophilic attack, f_k^- for nucleophilic attack) was calculated to investigate the reactive sites of the chelating membrane. In addition, the amounts of charge transfer (ΔN), the adsorption energy (ΔE_{ads}), and the Gibbs free energy of adsorption (ΔG_{ads}) of the metal ions with APTMS-DTPA ligand of the chelating membrane were also calculated.

2. Materials and methods

2.1. Chemicals and reagents

PVDF powders were provided by Chen Guang Co., Ltd (Chengdu, China) with a molecular weight of ca. 400,000. Analytical grade of polyvinyl pyrrolidine (PVP) as the pore-forming additive, dimethylsulfoxide (DMSO) as the solvent, diethylenetriaminepentaacetic acid (DTPA), and 3-aminopropyltrimethoxysilane (APTMS) were used for the preparation of the chelating membrane. The analytical grade of reagents including $NiSO_4{\cdot}6H_2O$, $CaCl_2$, NH_4Cl, lactic acid, and citric acid were used as received. A stock Ni(II) solution with the concentration of 1,000 mg/l was prepared by dissolving weighed amounts of $NiSO_4{\cdot}6H_2O$ in deionized water. The working solutions were prepared by diluting the stock solutions to appropriate volumes. The concentrations of stock solutions containing the existent cation and organic acid were 0.1 and 0.2 mol/l, respectively. The above-mentioned chemical reagents were supplied by Jingchun Scientific Co., Ltd (Shanghai, China).

2.2. Preparation of the PVDF-based chelating membrane

DTPA (2 g) and APTMS (1.92 g) were mixed in 30 ml DMSO. The mixture was heated to 393 K for 30 min to form the covalent amide bond between DTPA and APTMS. Then, the solution was cooled to 353 K. At the same time, PVDF (5 g) and PVP (0.7 g) were added to this solution and then agitated for 5 h with the temperature in the range of 343–353 K. The PVDF-based chelating membrane was obtained via a phase inversion technique with deionized water as the

nonsolvent. Finally, the membrane with thickness of 350 μm was left for subsequent characterization and adsorption experiments.

2.3. Membrane characterization

An environmental scanning electron microscopy (Philips XL30, Amsterdam, Netherlands) was employed to analyze the surface morphology of the chelating membrane. The E55+FRA106 FTIR spectrometer (Bruker Inc., Karlsruhe, Germany) was adopted to examine the FTIR spectra of the chelating membrane before and after Ni(II) was loaded. A nuclear magnetic resonance spectrometer (Bruker Avance III 400, Karlsruhe, Germany) was also used to characterize the chemical groups of the chelating membrane. The mean pore size of the chelating membrane was characterized by water permeability method [19]. Point of zero charge (pH_{pzc}) of the membrane was measured using a batch equilibration method [20].

2.4. Adsorption experiments

All the adsorption experiments were performed by a static batch method [13]. The flat-sheeted membrane with the area of 78.5 cm^2 was dipped into 200 ml solution containing Ni(II). The solutions were pH-adjusted using HAC-NaAC buffer solutions. The effects of pH, initial Ni(II) concentration, contact time, and temperature were studied by a set of adsorption tests. The concentration of Ni(II) was measured using the WFX-110 atomic absorption spectrometer (Rayleigh Analytical Instrument Co., Ltd., Beijing, China). The amount of Ni(II) adsorbed onto the chelating membrane was calculated as follows [13,21]:

$$q_t = \frac{(c_0 - c_t) \times V}{A} \tag{1}$$

where q_t is the amount of Ni(II) adsorbed onto a unit area of the membrane (mg/cm^2) at time t. c_0 and c_t (mg/l) are the concentrations of Ni(II) in the aqueous solution at the initial time and time t, respectively. c_t and q_t are described as equilibrium concentration (c_e) and equilibrium absorbing capacity (q_e), when the adsorption equilibrium is evidenced. V is the volume of the aqueous phase (l), and A is the surface area of the membrane (cm^2).

Herein, for the following experimental studies, pH of the solutions was maintained the optimum value derived from the above-mentioned experimental result of pH effect. Adsorption kinetics for the single Ni(II) aqueous solution was investigated at 298 K, and the initial Ni(II) concentration was 50 mg/l. The adsorption isotherm of the single Ni(II) system was also examined at 298 K with different initial Ni(II) concentrations (20–140 mg/l).

In order to elucidate the interferences of Ca(II) and NH_4^+, the nickel uptakes of the chelating membrane were measured with different cation concentrations (0–5 mmol/l). For the removal of nickel in the form of metal/organic acid complexes, lactic acid and citric acid with the concentrations in the range of 0–10 mmol/l were chosen as the chelating agents. Adsorption kinetics and adsorption isotherms of the chelating membrane toward Ni(II) with the presence of Ca(II), NH_4^+, lactic acid, and citric acid were also studied at 298 K, by the same method as that of the single Ni(II) system. The solutions with Ni(II) of 50 mg/l and the temperature at 298 K were used in the above experiments. The additions of the coexistent cation and organic acid were controlled at 1 and 10 mmol/l, respectively.

2.5. Computational details

All the calculations are based on the DFT and were performed with Materials Studio DMol^3 package (version 4.1, Accelrys Inc., San Diego, USA) [22]. The structural optimization was performed at the generalized gradient approximation level with the spin unrestricted approach. The double numerical plus polarization functions and the Becke exchange functional in conjunction with the Lee–Yang–Parr correlation functional (BLYP) were employed. All calculations employed a method based on Pulay's direct inversion of iterative subspace technique to accelerate SCF convergence, and a small electron thermal smearing value of 0.005 Ha was used. The structure of APTMS-DTPA ligand of the chelating membrane is shown in Fig. 1, considering the simplification of DFT simulations. The geometry of NH_4^+ in the form of $[NH_4(H_2O)_4]^+$ was considered. The calculated configurations of Ni(II), Ca(II), lactic acid, and citric acid could be found in our previous research [3].

Within the conceptual framework of DFT, the chemical potential (μ), the global hardness (η) and the electrophilicity index (ω) were defined as Eqs. (2)–(4) [15,23], respectively.

$$\mu = \frac{(E_{HOMO} + E_{LUMO})}{2} \tag{2}$$

$$\eta = \frac{(E_{LUMO} - E_{HOMO})}{2} \tag{3}$$

$$\omega = \frac{\mu^2}{2\eta} \tag{4}$$

where E_{HOMO} and E_{LUMO} are the energies of the highest occupied and the lowest unoccupied molecular

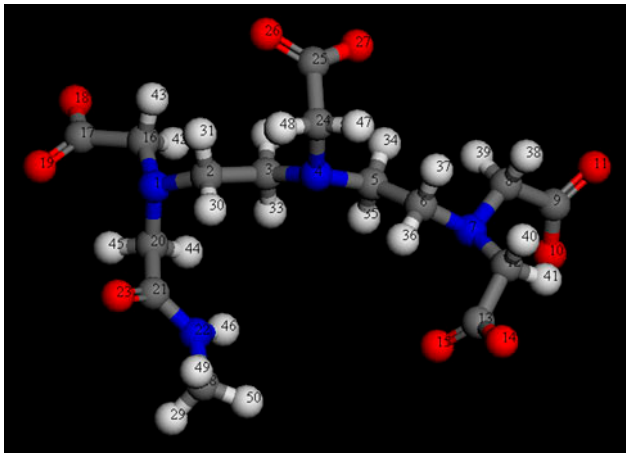

Fig. 1. Optimized structure of APTMS-DTPA ligand with the atoms numbering scheme adopted in this study. Atom types are denoted by sequence number as follows: 29∼50-hydrogen; 2, 3, 5, 6, 8, 9, 12, 13, 16, 17, 20, 21, 24, 25, 28-carbon; 10, 11, 14, 15, 18, 19, 23, 26, 27-oxygen; 1, 4, 7, 22-nitrogen.

orbitals (HOMO and LUMO), respectively. The parameters of μ, η, and ω are related to the properties of an isolated reactant; however, the interactions of the APTMS-DTPA ligand with Ni(II), Ca(II), and NH_4^+ and that of lactic acid and citric acid with Ni(II) can be represented by the parameter of charge transfer (ΔN). ΔN was defined by Eq. (5) [24]:

$$\Delta N = \frac{\mu_B - \mu_A}{2(\eta_A + \eta_B)} \tag{5}$$

where μ_A, μ_B, η_A, and η_B are the chemical potential and chemical hardness of the reactants A and B, respectively. The condensed FF is helpful to describe the reactivity of an atom in a reactant. Thus, for an atom k in a reactant, two kinds of condensed FF, namely f_k^+ and f_k^- can be obtained. The site that has the maximum value of f_k^+ and f_k^- can be considered as the active site corresponding to the nucleophile attack and electrophile attack, respectively. The value of condensed FF for APTMS-DTPA ligand of the chelating membrane was calculated using the Mulliken population analysis. The Mulliken atomic charges were assessed by the technique of electrostatic potential derived charges.

For the study of metal–organic complexes, the core treatment pattern used for all complexes is effective core potentials. The geometries of metal–organic complexes were optimized, and the convergence criteria for geometry optimization were the default threshold values. A continuum solvation model (COSMO) was used, and the dielectric constant of water was set as 78.54. Frequency calculations and Mulliken population analyses were performed to obtain the geometrical and energetic parameters of the metal-organic complexes. The adsorption energy (ΔE_{ads}, kJ/mol) and Gibbs free energy of adsorption (ΔG_{ads}, kJ/mol) at 298 K were calculated according to Eqs. (6) and (7) [3]:

$$\Delta E_{ads} = E(ML^{2-}) + 6E(H_2O) - E(L^{4-}) - E(M(H_2O)_6)^{2+}) \tag{6}$$

$$\Delta G_{ads} = \Delta E_{ads} + G(ML^{2-}) + 6G(H_2O) - G(L^{4-}) - G(M(H_2O)_6)^{2+}) \tag{7}$$

where E(X) is the COSMO-corrected total energy of species (X). M and L refer to metal and ligand, respectively. G(X) is the computed temperature-corrected free energy of species (X) at 298 K.

3. Results and discussion

3.1. Characterization of the chelating membrane

3.1.1. SEM analysis

The surface morphology of APTMS-DTPA/PVDF chelating membrane is shown in Fig. 2. As shown in Fig. 2, the chelating membrane possesses a uniform microporous structure as the virgin PVDF membrane [25]. In comparison with the virgin PVDF membrane with the mean pore size of 0.22 μm, the mean pore size of the chelating membrane reduces to 0.18 μm. The chelating membrane still maintains the microstructure; nevertheless, this porous microstructure is found to be partially blocked because of the resultant colloidal substances during the preparation process.

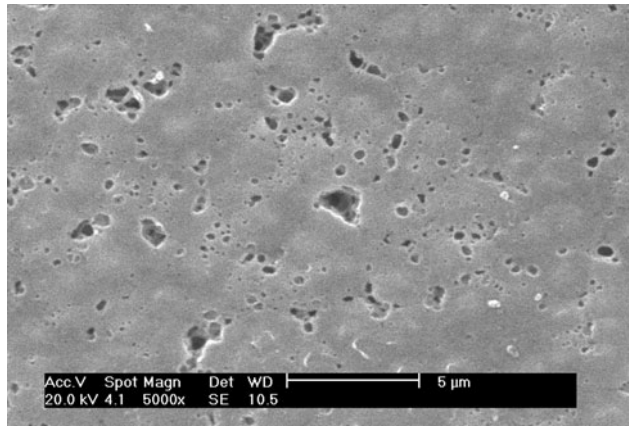

Fig. 2. Surface morphology of APTMS-DTPA/PVDF chelating membrane.

3.1.2. FTIR analysis

The FTIR spectra of the virgin PVDF membrane and the chelating membrane before and after Ni(II) adsorption are shown in Fig. 3. As shown in Fig. 3, the peaks appearing at 471, 1,200, and 3,025 cm^{-1} derive from C–F wagging, bending, and stretching vibration of PVDF polymer [26], respectively. For the spectrum of APTMS-DTPA/PVDF membrane (curve b), the peaks at 1,535 and 1,647 cm^{-1} can be assigned to N–H bending of bridging secondary amine and acylamide groups [13], respectively. After Ni(II) adsorption (curve c), the increasing intensity of peak at 600 cm^{-1} indicates the formation of Ni–N bond [27,28]. Also, the increasing intensities of the peaks at 1,071 and 1,637 cm^{-1}, and the decreasing intensity of the peak at 690 cm^{-1} are indicative that nitrogen atoms of DTPA are sites for chelation [13]. In order to reveal the change of carboxyl group of APTMS-DTPA ligand after Ni(II) was loaded, the FTIR spectra of the APTMS-DTPA colloid compound and its nickel-loaded form were also supplied as an inset in Fig. 3. The peak at 1,399 cm^{-1} can be attributed to carboxylic in plane O–H bending [13]. After Ni(II) adsorption, the peak shifts to 1,403 cm^{-1} and the intensity of its also decreases, due to carboxylic O–H coordinating with Ni(II). Thus, during the adsorption process, the chemical chelation between Ni(II) and the chelating membrane is confirmed.

3.1.3. NMR analysis

The ^{13}C solid-state NMR spectra of APTMS-DTPA/PVDF membrane before and after Ni(II) adsorption were measured, and the tested spectra were shown in Fig. 4. As indicated in Fig. 4, the peak at 31.1 ppm originates from adamantane which is used as the internal standard. The $–CH_2–$ and $–CF_2–$ carbons of the PVDF main chains contribute to the peaks at 44.6 ppm and 121.8 ppm [29]. For the spectra (curves *a* and *b*), the peaks at 10.9, 21.9, and 50.3 ppm can be assigned to α and β carbons of $–CH_2–$ groups [30,31], and $–OCH_3$ group [32] of APTMS ($(H_3CO)_3Si–CH_2(\alpha)–CH_2(\beta)–CH_2(\gamma)–NH_2$), respectively. The peak appearing at 59.1 ppm is assigned to $–CH_2N–$ carbon of DTPA and the peak at 169.8 ppm can be attributed to the carboxylic and acylamide groups of APTMS-DTPA compounds. After Ni(II) adsorption, the new peak appearing at 165.5 ppm, the increasing intensity at 59.1 ppm, and the decreasing peak at 169.8 ppm indicate that the nitrogen atoms of $–CH_2N–$ groups and oxygen atoms of carboxylic groups are chelated by Ni(II) [13,28]. Therefore, it can be assumed that the $–CH_2N–$ and carboxylic groups pertaining to DTPA coordinate to Ni(II), thereby forming the $Ni(APTMS-DTPA)^{2-}$ complex.

3.2. Effect of variables

3.2.1. Effects of pH, initial Ni(II) concentration, contact time and temperature

The influence of pH ranging from 2.5 to 7.5 on the adsorption property of the APTMS-DTPA/PVDF chelating membrane is shown in Fig. 5. As can be noticed, with increasing pH value, the higher Ni(II) uptake can be obtained. The tested pH_{pzc} of the chelating membrane is 6.7, and the optimum pH for Ni(II) adsorption is located at 6.7. When pH exceeds 7, the Ni(II) uptake decreases because Ni(II) starts to precipitate as $Ni(OH)_2$. At lower pH values, the oxygen and nitrogen atoms for chelation are protonated and the H^+ ions compete with Ni(II), which do not favor the chelating process because of the electrostatic

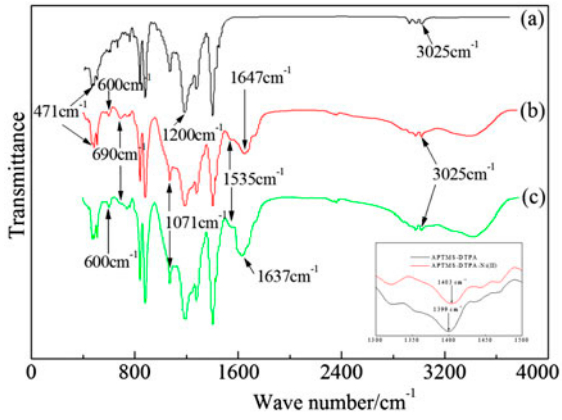

Fig. 3. FTIR spectra: (a) the virgin PVDF membrane; (b) APTMS-DTPA/PVDF chelating membrane; (c) Ni(II)-loaded chelating membrane.

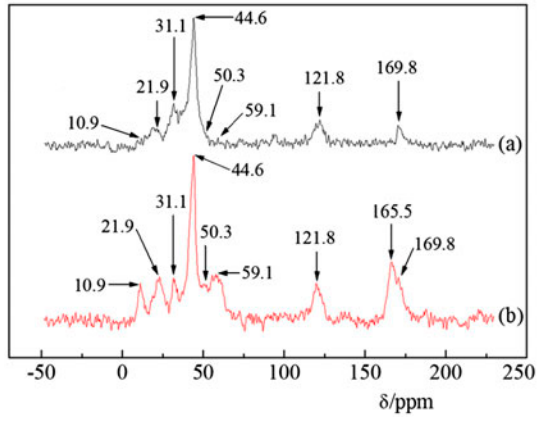

Fig. 4. ^{13}C solid-state NMR spectra: (a) APTMS-DTPA/PVDF chelating membrane; (b) Ni(II)-loaded chelating membrane.

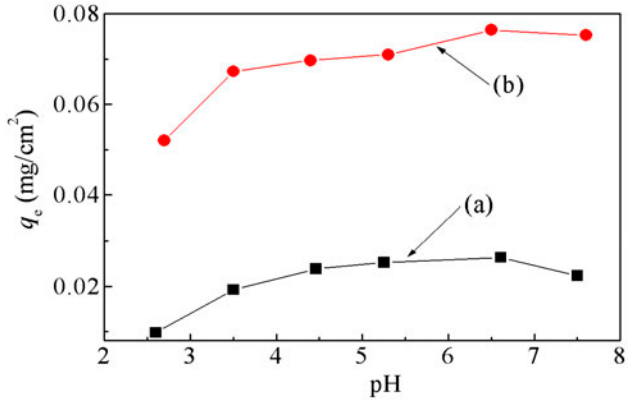

Fig. 5. Effect of pH on the chelating membrane toward Ni (II): (a) MA-DTPA/PVDF membrane (c_0(Ni) = 50 mg/l; t: 300 min; membrane area: 157 cm^2; temperature: 298 K); (b) APTMS-DTPA/PVDF membrane (c_0(Ni) = 50 mg/l; t: 300 min; membrane area: 78.5 cm^2; T: 298 K).

repulsion. When pH increases, the adsorption process of Ni(II) uptake tends to occur with the deprotonated functional groups of the membrane.

The Ni(II) uptake of the chelating membrane varying the initial Ni(II) concentration is shown in Fig. 6. As the concentration of Ni(II) increases, the metal uptake increases significantly. When Ni(II) concentration varies from 20 to 140 mg/l, the Ni(II) uptake of APTMS-DTPA/PVDF membrane increases from 0.0398 to 0.1052 mg/cm^2. However, the removal of Ni (II) reduces from 78 to 30%. As indicated in Figs. 5 and 6, in comparison with MA-DTPA/PVDF chelating membrane (curves a) [13], the APTMS-DTPA/PVDF chelating membrane shows a much higher uptake of Ni(II). When the concentration of Ni(II) is 50 mg/l, the metal uptake of MA-DTPA/PVDF membrane is 0.0264 mg/cm^2, which is 34.5% as that of APTMS-DTPA/PVDF membrane. Therefore, APTMS-DTPA/PVDF membrane has a stronger affinity for Ni(II) than MA-DTPA/PVDF membrane.

The Ni(II) uptakes of APTMS-DTPA/PVDF membrane as a function of time at different temperatures are shown in Fig. 7. As inferred from Fig. 7, the time required to achieve equilibrium for APTMS-DTPA/PVDF membrane is 300 min. Two stages, including rapid and slow stage, occur in the adsorption process. The rapid stage extends for the first 180 min while the slow adsorption for the remaining 120 min. It also can be seen in Fig. 7, for the rapid adsorption process, the high temperature accelerates the transportation of Ni (II), so Ni(II) uptakes of the membrane at 298 and 308 K are slightly larger than that of 288 K. In the remaining time, the adsorption capacity of the chelating membrane decreases with the increase in temperature, which indicates that the adsorption process is exothermic. However, the temperature does not exert a significant influence on the adsorption property of the membrane because of the unconspicuous differences of Ni(II) uptakes among the three temperatures.

3.2.2. *Effects of Ca(II) and NH_4^+*

APTMS-DTPA/PVDF chelating membrane tends to bind almost the existent cations owing to its high complexing capability. Therefore, the existent cations can occupy the active sites for complexation to compete with Ni(II). Ca(II) is a conventional cation of the solution, and NH_4^+ can also coexist with Ni(II) because ammonium acid fluoride has been always used as an accelerator in the process of nickel electroless plating.

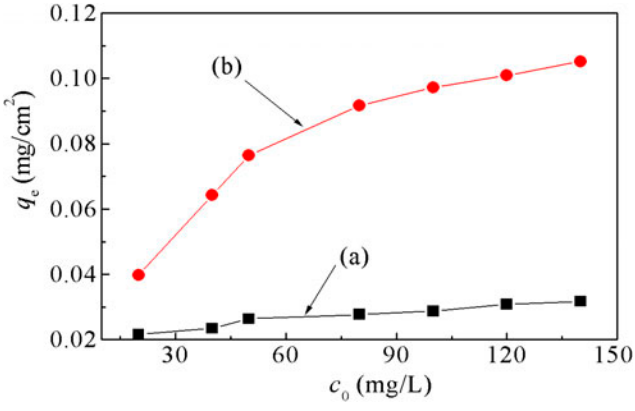

Fig. 6. Effect of initial Ni(II) concentration on the chelating membrane toward Ni(II): (a) MA-DTPA/PVDF membrane (t: 300 min; membrane area: 157 cm^2; temperature: 298 K; pH: 6.6); (b) APTMS-DTPA/PVDF (t: 300 min; membrane area: 78.5 cm^2; T: 298 K; pH: 6.7).

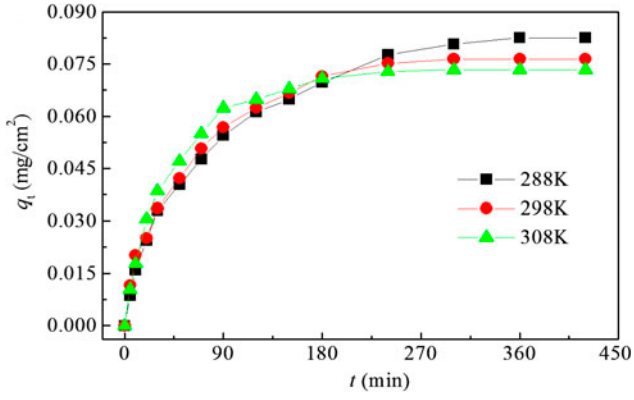

Fig. 7. Effects of contact time and temperature on APTMS-DTPA/PVDF chelating membrane toward Ni(II): c_0(Ni) = 50 mg/l; membrane area: 78.5 cm^2; pH: 6.7.

The Ni(II) uptakes of the membrane varying the concentrations of Ca(II) and NH_4^+ are described in Fig. 8. As the concentrations of the cations increase from 0 to 5 mmol/l, the Ni(II) uptakes of APTMS-DTPA/PVDF membrane decrease. The existent Ca(II) and NH_4^+ with the concentration of 1 mmol/l reduce Ni(II) uptake of the membrane by 5.2 and 3.2%, respectively. Therefore, the existent Ca(II) and NH_4^+ compete with Ni(II) for occupying the adsorption sites. Nevertheless, the chelating membrane shows a higher affinity for Ca(II) than NH_4^+. With the presence of the competitive cations, however, the Ni(II) uptake of APTMS-DTPA/PVDF membrane still predominates the adsorption process. Under the same experimental condition, it should be mentioned that the existent Ca (II) and NH_4^+ with the concentration of 1 mmol/l reduce the Ni(II) uptake of MA-DTPA/PVDF membrane by 24 and 15% [3], respectively. The negative influences of the coexistent cations on Ni(II) adsorption of APTMS-DTPA/PVDF membrane are less notable than that of MA-DTPA/PVDF membrane. Therefore, it can be deduced that APTMS-DTPA/PVDF chelating membrane has a high applied value of metal recovery.

3.2.3. Effects of lactic acid and citric acid

The complexing reagents, including lactic acid and citric acid, have been widely used in the nickel electroless plating industries. The existent organic acids can hamper the adsorption process, because Ni(II) is easily coordinated by the organic acids. The influences of lactic acid and citric acid with different concentrations on Ni(II) uptakes of the chelating membrane are shown in Fig. 9. As shown in Fig. 9, the Ni(II) uptake of the chelating membrane reduces with the increasing concentration of the organic acid. This may be because all the nickel ions are complexed, and the complexed form of Ni(II) affects the metal uptake of the chelating membrane to some extent. When lactic acid and citric acid exist with the concentration of 1 mmol/l, the Ni(II) uptake of APTMS-DTPA/PVDF membrane decreases by 2.4 and 4.8%, respectively. The facts mentioned previously suggest the order of complexing capability associated with the size of the ligands is lactic acid < citric acid [3].

3.3. Adsorption characteristic studies

3.3.1. Adsorption kinetics

To describe the adsorption kinetics of APTMS-DTPA/PVDF chelating membrane toward Ni(II), the experimental data were fitted to three commonly mathematical equations, namely Lagergren first-order equation, Lagergren second-order equation, and intraparticular diffusion model [33–35]. The Ni(II) uptakes as a function of time for the Ni(II)–Ca(II) and Ni(II)–NH_4^+ systems are presented in Fig. 10. Compared with the single Ni(II) system (Fig. 7), the nickel uptakes decrease with the coexistence of Ca(II) and NH_4^+. On the basis of this, it is apparent that Ca(II) and NH_4^+ compete with Ni(II) for the adsorption sites. The amounts of Ni(II) adsorbed onto the chelating membrane as a function of time for the coexistent com-

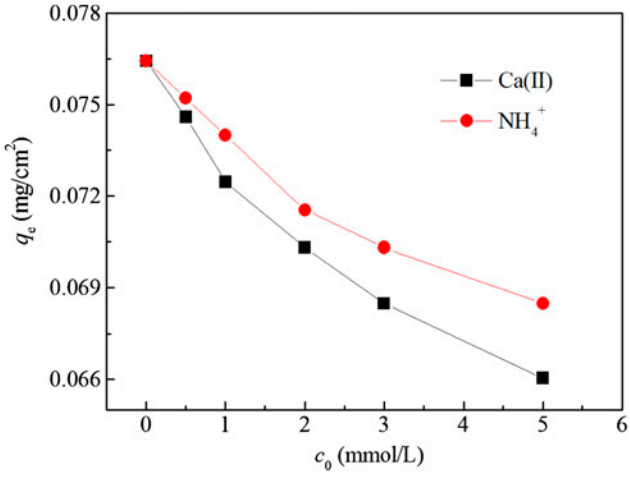

Fig. 8. Effect of the existent cation concentration on APTMS-DTPA/PVDF chelating membrane toward Ni(II): c_0(Ni) = 50 mg/l; t: 300 min; membrane area: 78.5 cm^2; T: 298 K; pH: 6.7.

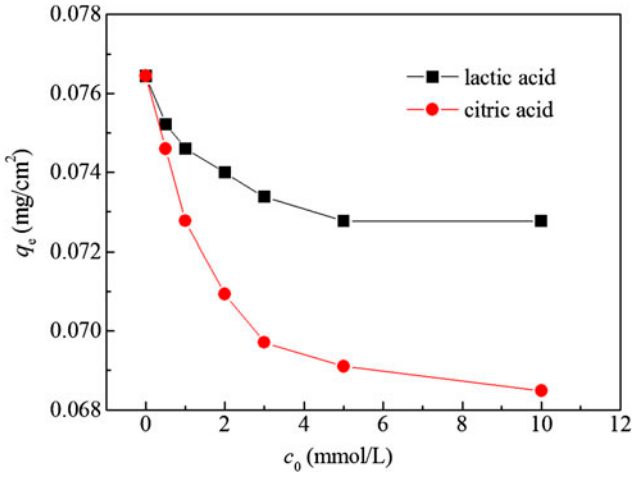

Fig. 9. Effect of the existent complexing reagent concentration on APTMS-DTPA/PVDF chelating membrane toward Ni(II): c_0(Ni) = 50 mg/l; t: 300 min; membrane area: 78.5 cm^2; T: 298 K; pH: 6.7.

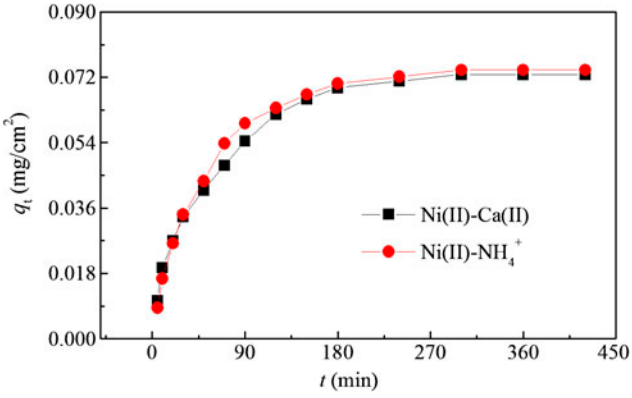

Fig. 10. Adsorption kinetics of APTMS-DTPA/PVDF chelating membrane toward Ni(II) for the cation coexisting systems: c_0(Ni) = 50 mg/l; c_0(Ca) = c_0(NH_4^+) = 1 mmol/l; T: 298 K; membrane area: 78.5 cm^2; pH: 6.7.

plexing reagent systems are shown in Fig. 11. As shown in Fig. 11, the Ni(II) uptake of the membrane for Ni(II)–lactic acid system is larger than that of Ni(II)–citric acid system.

Among the three kinetics models, Lagergren second-order model, with higher coefficient of determination ($R^2 > 0.99$) than Lagergren first-order and intraparticular diffusion models, gives an excellent description of the kinetics. The analyzed parameters of Lagergren second-order model for the single Ni(II) system, and the binary systems, including Ni(II)–Ca (II), Ni(II)–NH_4^+, Ni(II)–lactic acid, and Ni(II)–citric acid, are shown in Table 1. Where q_e is the amount of adsorbed Ni(II) (mg/cm^2) at equilibrium, and k_2 (cm^2/mg min^{-1}) is the rate constant.

As seen in Table 1, it can be concluded that the competitive adsorption of Ca(II) and NH_4^+ accelerates

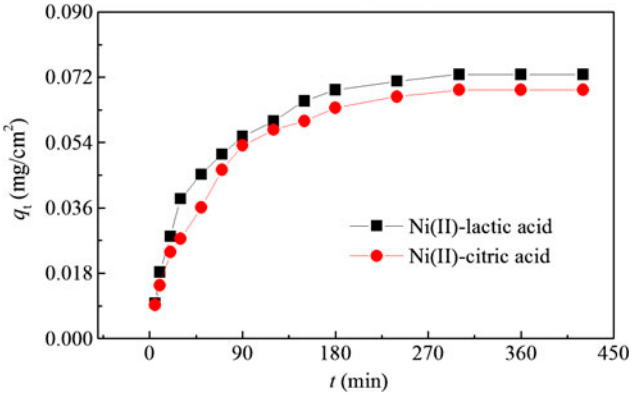

Fig. 11. Adsorption kinetics of APTMS-DTPA/PVDF chelating membrane toward Ni(II) for the complexing reagent coexisting systems: c_0(Ni) = 50 mg/l; c_0(lactic acid) = c_0(citric acid) = 10 mmol/l; T: 298 K; membrane area: 78.5 cm^2; pH: 6.7.

the adsorption process by examining the values of k_2. It is also reasonable to assume that the membrane exhibits a higher binding capability for Ca(II) than NH_4^+. For the Ni(II)-complexing reagent systems, as also indicated in Table 1, the values of k_2 are in the ascending order of lactic acid < citric acid, implying the larger interference of citric acid.

3.3.2. Adsorption isotherms

The thermodynamic behavior of the chelating membrane toward Ni(II) is analyzed by Freundlich, Langmuir and Dubinin–Radushkevich (D–R) isotherm models [36,37]. Adsorption isotherms of the single Ni(II) system, and the Ni(II)–Ca(II), Ni(II)–NH_4^+, Ni(II)–lactic acid, and Ni(II)–citric acid binary systems are shown in Figs. 12 and 13.

By the comparison of the determination coefficients ($R^2 > 0.99$), Langmuir isotherm model gives a better description of the thermodynamic behavior than Freundlich and D–R isotherm models. The analyzed parameters of the Langmuir isotherm model are also listed in Table 1, where q_m (mg/cm^2) is the maximum adsorption capacity at equilibrium, and parameter b (l/mg) is related to the adsorption affinity.

Because of the unoccupied adsorption sites, the calculated maximum adsorption capacity (q_m) is slightly greater than the experimental value. The Langmuir parameter b associated with the adsorption affinity for the cation coexistent system is in the order of Ni(II)–Ca(II) < Ni(II)–NH_4^+, reflecting the higher interferential effect of Ca(II). Similarly, the parameter b is in the descending order for the Ni(II)–lactic acid and Ni(II)–citric acid acid binary mixtures, indicating that citric acid shows a more significant influence on Ni(II) adsorption than lactic acid. It should be noticed that the mean free energy of adsorption analyzed by D–R isotherm model for all adsorption systems mentioned previously varies in the range of 8–16 kJ/mol, suggesting the chemisorption characteristic of Ni(II) adsorption [13,37].

3.3.3. Thermodynamic parameters

The capacity of the chelating membrane toward Ni (II), and the adsorption mechanism of the membrane can be evaluated based on the thermodynamic parameters involving standard free energy change (ΔG°), standard enthalpy change (ΔH°), and standard entropy change (ΔS°) [38]. ΔG°, ΔH°, and ΔS° were calculated [39] and summarized in Table 2. It can be seen from Table 2 that the values of ΔH° are negative, indicating the exothermic nature of the adsorption

Table 1
Adsorption parameters of Lagergren second-order model and Langmuir model at 298 K

System	Lagergren second-order model			Langmuir model		
	k_2 ($cm^2/mg\,min^{-1}$)	q_e (mg/cm^2)	R^2	q_m (mg/cm^2)	b (l/mg)	R^2
Single Ni(II)	0.3514	0.0764	0.9972	0.1388	0.2056	0.9957
Ni(II)–Ca(II)	0.4761	0.0728	0.9978	0.1102	0.1164	0.9960
Ni(II)–NH_4^+	0.3935	0.0740	0.9986	0.1128	0.1418	0.9954
Ni(II)–lactic acid	0.3781	0.0728	0.9966	0.1198	0.1490	0.9902
Ni(II)–citric acid	0.4410	0.0678	0.9974	0.1122	0.0734	0.9983

process. The positive change of ΔS° shows the increasing randomness during the adsorption process, in which the hydrated nickel ions tend to liberate water molecules. This liberation is essential for the occurrence of the chelating reaction, promoting the disorder of the system. ΔG° with a negative value indicates that the adsorption process is spontaneous.

Based on the analyses mentioned above, the performance of APTMS-DTPA/PVDF chelating membrane toward Ni(II) was confirmed. Furthermore, The coexistent Ca(II), NH_4^+, lactic acid, and citric acid show the interferential effects on the Ni(II) uptake of the membrane. To further reveal the influences of the coexistent cations and organic acids on the chelating membrane toward Ni(II), the DFT calculations were performed.

3.4. DFT simulation

3.4.1. The chemical reactivity descriptors

The calculated energies of HOMO, LUMO, and the band gaps ($\Delta E_{LUMO\text{-}HOMO}$) of APTMS-DTPA ligand, Ni(II), Ca(II), NH_4^+, lactic acid, and citric acid are shown in Table 3. Among the above-mentioned reactants, Ni(II) has the lowest LUMO energy and APTMS-DTPA ligand has the highest HOMO energy. Thus, Ni(II) and APTMS-DTPA ligand show the stronger abilities of accepting and donating electrons than other reactants. The difference between E_{LUMO} of Ni (II) and E_{HOMO} of APTMS-DTPA ligand, described as $\Delta E(LUMO_{Ni(II)}–HOMO_{APTMS\text{-}DTPA})$, is 0.0022 au, which is smaller than $\Delta E(LUMO_{Ca(II)}–HOMO_{APTMS\text{-}DTPA})$, $\Delta E(LUMO_{NH_4^+}–HOMO_{APTMS\text{-}DTPA})$, $\Delta E(LUMO_{Ni(II)}–HOMO_{lactic\ acid})$ and $\Delta E(LUMO_{Ni(II)}–HOMO_{citric\ acid})$. So, we believe that the chelation between Ni(II) and APTMS-DTPA ligand is notable.

The calculated values of the global reactivity descriptors for APTMS–DTPA ligand, Ni(II), Ca(II), NH_4^+, lactic acid, and citric acid are also shown in Table 3. The values of chemical potential (μ) of Ni(II), Ca(II), and NH_4^+ are more negative than that of APTMS-DTPA ligand, lactic acid, and citric acid. Therefore, Ni(II), Ca(II), and NH_4^+ act as the electrophiles (electron acceptors); however, APTMS-DTPA ligand, lactic acid, and citric acid serve as the nucleophiles (electron donors). Among the three electrophiles, the electronegativity (χ, $\chi = -\mu$) decreases in the order of Ni(II) > Ca(II) > NH_4^+. It can be inferred that Ni(II) obtains the electrons form APTMS-DTPA ligand more easily than Ca(II) and NH_4^+. For the aforementioned electrophiles, the computed hardness (η) decreases in the order of NH_4^+ > Ca(II) > Ni(II), which also shows that Ni(II) owns the higher reactivity of accepting electrons than Ca(II) and NH_4^+.

The calculated electrophilicity index (ω) of Ni(II), Ca(II), and NH_4^+ is larger than that of APTMS-DTPA ligand, lactic acid, and citric acid, consistent with the analysis of chemical potential. Among the electrophiles, ω lines in the order of Ni(II) > Ca(II) > NH_4^+, indicating that Ni(II) has an obvious capacity of accepting electrons from the nucleophiles. Furthermore, it also can be deduced that the interferential effect of Ca(II) on Ni(II) adsorption is more notable than that of NH_4^+. It should be noted that the values of μ and ω for the nucleophiles do not follow the order of lactic acid > citric acid > APTMS-DTPA ligand, and η is also not in the order of lactic acid < citric acid < APTMS-DTPA ligand, which suggests that the aforementioned three nucleophiles may act as the electrophiles in other reacting processes.

In comparison with the intramolecular parameters involving chemical potential, hardness and electrophilicity index, the descriptor of charge transfer (ΔN) will be helpful to get a complete picture of the adsorption process. The high absolute value of ΔN indicates the strong interaction of reactants [24]. The amounts of charge transfer of Ni(II), Ca(II), NH_4^+ with APTMS-DTPA ligand and that of Ni(II) with lactic acid and citric acid are shown in Table 4. The negative values of ΔN indicate that Ni(II), Ca(II), and NH_4^+ act as the electrophiles, while APTMS-DTPA ligand, lactic acid, and citric acid act as the nucleophiles. The amount of

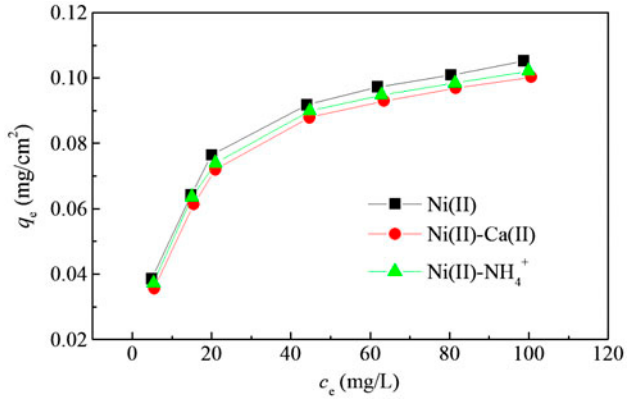

Fig. 12. Adsorption isotherm of APTMS-DTPA/PVDF chelating membrane toward Ni(II) for the cation coexisting systems: c_0(Ni) = 50 mg/l; c_0(Ca) = c_0(NH_4^+) = 1 mmol/l; *t*: 300 min; *T*: 298 K; membrane area: 78.5 cm^2; pH: 6.7.

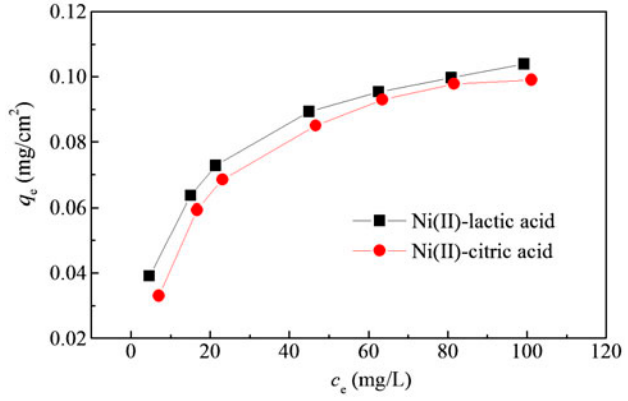

Fig. 13. Adsorption isotherm of APTMS-DTPA/PVDF chelating membrane toward Ni(II) for the complexing reagent coexisting systems. c_0(Ni) = 50 mg/l; c_0(lactic acid) = c_0(citric acid) = 10 mmol/l; *t*: 300 min; *T*: 298 K; membrane area: 78.5 cm^2; pH: 6.7.

charge transfer between Ni(II) and APTMS-DTPA ligand ($\Delta N_{\text{APTMS-DTPA}\rightarrow\text{Ni(II)}}$) is 1.98, 4.75, 1.35, and 1.24 times as that of $\Delta N_{\text{APTMS-DTPA}\rightarrow\text{Ca(II)}}$, $\Delta N_{\text{APTMS-DTPA}\rightarrow NH_4^+}$, $\Delta N_{\text{lactic acid}\rightarrow\text{Ni(II)}}$, and $\Delta N_{\text{citric acid}\rightarrow\text{Ni(II)}}$, respectively. Hence, during the adsorption process, the chelating membrane bearing the APTMS-DTPA ligand, shows a higher affinity for Ni(II) than Ca(II) and NH_4^+. In comparison with the value of ΔN between NH_4^+ and APTMS-DTPA ligand ($\Delta N_{\text{APTMS-DTPA}\rightarrow NH_4^+}$), the higher absolute value of $\Delta N_{\text{APTMS-DTPA}\rightarrow\text{Ca(II)}}$ shows that the interferential effect of Ca(II) on Ni(II) uptake is more remarkable than that of NH_4^+. Similarly, we can conclude that citric acid exerts a more negative effect on Ni(II) adsorption than lactic acid. However, these two kinds of organic acids show the smaller affinities for Ni(II) than APTMS-DTPA ligand of the membrane.

3.4.2. The complexing sites of APTMS-DTPA ligand

The DFT descriptors discussed above cannot tell the complexing sites of the chelating membrane. However, the chelation between APTMS-DTPA ligand and Ni(II) can be explained well with the help of condensed FF. Ni(II) ion has a maximum coordination number of six and may adopt an octahedral complexing arrangement. The APTMS-DTPA ligand can provide eight complexing sites, namely N_1, N_4, N_7, O_{10}, O_{14}, O_{18}, N_{22}, and O_{27} atoms (Fig. 1). In this regard, two complexing sites of the chelating membrane will be spared.

The calculated f_k^-, f_k^+ and atomic charge of the above-mentioned eight complexing sites are listed in Table 5. The negative FF value can be assigned that the electron density is depleted or accumulated from a particular site [15]. In the process of Ni(II) adsorption, APTMS-DTPA ligand of the chelating membrane acts as a nucleophile; therefore, the complexing sites of the membrane should have the high values of f_k^- and the negative values of atomic charge. It can be seen from the data of Table 5, the nucleophilic characteristics of the eight sites decrease in the order of $O_{27} > N_4 > N_7 = O_{14} > N_1 > O_{10} > O_{18} > N_{22}$, indicating O_{18} and N_{22} atoms will not be chelated by Ni(II). The optimized geometry of Ni (APTMS-DTPA)$^{2-}$ complex with the minimum energy is shown in Fig. 14. The optimized geometrical parameters of this kind of Ni (APTMS-DTPA)$^{2-}$ complex (bond length in Å and bond angle in degree) are shown in Table 6. Obviously, the Jahn–Teller distortion leads to an elongated octahedral configuration of Ni (APTMS-DTPA)$^{2-}$ complex.

3.4.3. The adsorption energy and Gibbs free energy of adsorption

The adsorption energy (ΔE_{ads}) and the Gibbs free energies of adsorption (ΔG_{ads}) for the Ni(II)–, Ca(II)–, NH_4^+–(APTMS-DTPA) complexes were assessed, and the data are shown in Table 7. ΔE_{ads} indicates the complexing ability of the chelating ligand toward the cation; ΔG_{ads} can reflect the spontaneous trend of the reaction. The calculated ΔE_{ads} of the three metal-(APTMS-DTPA) complexes follows the order of Ni(II)–(APTMS-DTPA) < Ca(II)–(APTMS-DTPA) < NH_4^+–(APTMS-DTPA), indicating that the APTMS-DTPA ligand has a more notable affinity for Ni(II) than Ca(II) and NH_4^+. The negative value of ΔG_{ads} shows the spontaneous characteristic of the adsorption process. The adsorption of Ca(II) is due to the formation of metal complex of Ca (APTMS-DTPA)$^{2-}$, while the ion exchange plays a role in the NH_4^+ adsorption by means of the electrostatic relationship.

Table 2
Adsorption thermodynamic parameters of the chelating membrane toward Ni(II) at 298 K

System	ΔS°/(kJ/mol K)	ΔH°/(kJ/mol)	ΔG°/(kJ/mol)	R^2
Single Ni(II)	0.0656	−10.36	−27.91	0.9918
Ni(II)–Ca(II)	0.0538	−13.02	−30.05	0.9993
Ni(II)–NH_4^+	0.0548	−12.91	−29.24	0.9947
Ni(II)–lactic acid	0.0651	−11.92	−29.32	0.9943
Ni(II)–citric acid	0.0505	−13.92	−29.97	0.9942

Table 3
Calculated HOMO, LUMO, band gap ($\Delta E_{\text{LUMO-HOMO}}$), chemical potential ($\mu$), hardness ($\eta$), and global electrophilicity (ω) in au for APTMS-DTPA ligand and the existent cations and organic acids

Reactant	E_{HOMO}	E_{LUMO}	$\Delta E_{\text{LUMO-HOMO}}$	μ	η	ω
APTMS-DTPA	−0.1383	−0.0088	0.1295	−0.0736	0.0648	0.0418
Ni(II)	−0.2576	−0.1361	0.1215	−0.1968	0.0608	0.3189
Ca(II)	−0.3030	−0.0432	0.2598	−0.1731	0.1299	0.1153
NH_4^+	−0.2529	0.0198	0.2727	−0.1166	0.1364	0.0498
Lactic acid	−0.1757	0.0219	0.1976	−0.0769	0.0988	0.0299
Citric acid	−0.1585	−0.0312	0.1273	−0.0948	0.0635	0.0707

Table 4
Calculated charge transfer (ΔN) of APTMS-DTPA ligand to Ni(II), Ca(II) and NH_4^+ and that of lactic acid and citric acid to Ni(II)

Cation	APTMS-DTPA	Lactic acid	Citric acid
Ni(II)	−0.5073	−0.3759	−0.4099
Ca(II)	−0.2556	–	–
NH_4^+	−0.1068	–	–

Table 5
Calculated values of f_k^-, f_k^+ and atomic charge for the complexing atoms of APTMS-DTPA ligand

Atom	f_k^-	f_k^+	atomic charge
N_1	0.026	−0.006	−0.462
N_4	0.116	0.002	−0.501
N_7	0.028	0.000	−0.453
O_{10}	0.022	0.000	−0.692
O_{14}	0.028	0.001	−0.718
O_{18}	0.020	0.015	−0.712
N_{22}	0.001	0.078	−0.353
O_{27}	0.119	0.003	−0.693

Considering ΔE_{ads} of the Ni(II)–lactic acid and Ni (II)–citric acid complexes with values of −79.857 and −209.496 kJ/mol [3], the complexing abilities of lactic acid and citric acid toward Ni(II) cannot be comparable with that of APTMS-DTPA ligand. Therefore, we affirm that the APTMS-DTPA/PVDF chelating membrane deserves to be recommended for the treatment of nickel plating wastewater.

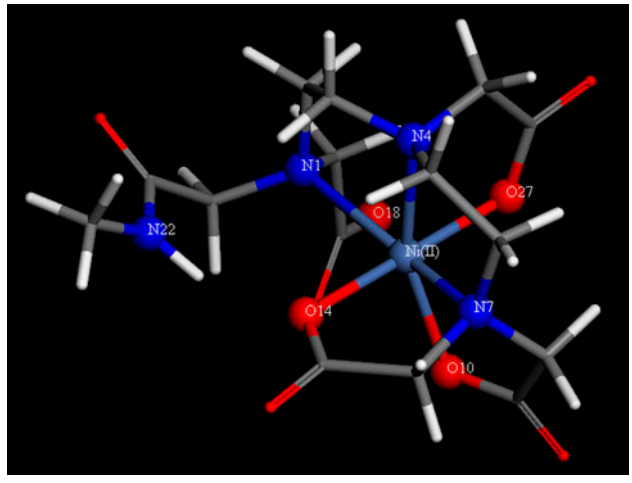

Fig. 14. Optimized structure of Ni(APTMS-DTPA)$^{2-}$ complex.

In this study, the influences of Ca(II), NH_4^+, lactic acid, and citric acid on Ni(II) adsorption of the APTMS-DTPA/PVDF chelating membrane were studied, using the experimental and DFT simulation methods.

Table 6
Optimized geometrical parameters of Ni (APTMS-DTPA)$^{2-}$ complex (lengths in Å and angles in degrees)

Ni–N_1	Ni–O_{14}	Ni–O_{27}	Angle $_{N4–Ni–N7}$	Angle $_{N1–Ni–O14}$	Angle $_{N1–Ni–N7}$
2.448	2.086	2.086	83.95	87.78	159.1

Table 7
Calculated adsorption energies and adsorbing Gibbs free energies for metal-(APTMS-DTPA) complexes

Complex	ΔE_{ads} (kJ/mol)	ΔG_{ads} (kJ/mol)
Ni (ATPMS-DTPA)$^{2-}$	−353.66	−569.20
Ca (ATPMS-DTPA)$^{2-}$	−286.32	−472.51
NH_4 (ATPMS-DTPA)$^{3-}$	−109.72	−68.923

However, it should be mentioned that other issues such as the investigation of Ni(II) uptake of the membrane in a continuous adsorption process, and the detailed analysis of difference in Ni(II) adsorption between APTMS-DTPA/PVDF and MA-DTPA/PVDF chelating membranes are also important. The above-mentioned unsolved issues will be investigated in the further research.

4. Conclusions

The APTMS-DTPA/PVDF chelating membrane was prepared to remove Ni(II) from the simulated wastewater. The influences of the existent Ca(II), NH_4^+, lactic acid, and citric acid on Ni(II) uptake of the chelating membrane were investigated using the batch adsorption experiments and the DFT simulations. The conclusions are shown as follows:

(1) The interferential influences of Ca(II) and citric acid on Ni(II) adsorption are more remarkable than that of NH_4^+ and lactic acid, respectively.
(2) Lagergren second-order model is competent for the description of the adsorption kinetics of the chelating membrane toward Ni(II), and the adsorption isotherms can be well described by Langmuir model. The adsorption of Ni(II) onto the chelating membrane is a spontaneous and exothermic process.
(3) Among the interactions of the cations and the complexing ligands of APTMS-DTPA/PVDF membrane, the chelation between Ni(II) and APTMS-DTPA ligand is most remarkable, because of the maximum charge transfer between them, and the more negative complexing energy and adsorbing Gibbs free energy of Ni(APTMS-DTPA)$^{2-}$ complex.
(4) In the adsorption process, the atoms of APTMS-DTPA ligand including N_1, N_4, N_7, O_{10}, O_{14}, and O_{27} are complexed by Ni(II); nevertheless, O_{18} and N_{22} atoms are not occupied.
(5) The interferential influences of Ca(II), NH_4^+, lactic acid, and citric acid on the Ni(II) uptake of APTMS-DTPA/PVDF chelating membrane have been confirmed. However, it should be mentioned that the coexistent cations and organic acids will not hamper the potential application of APTMS-DTPA/PVDF chelating membrane for recovering Ni(II) from the spent nickel plating solution.

Acknowledgement

This work was supported by Hebei Provincial Natural Science Foundation of China (Grant No. B2012203037). Also, we are very grateful to the editors and the reviewers for giving the valuable and instructive comments.

References

[1] K.E. Giller, E. Witter, S.P. Mcgrath, Toxicity of heavy metals to microorganisms and microbial processes in agricultural soils: A review, Soil Biol. Biochem. 30 (1998) 1389–1414.
[2] L. Wang, R.T. Liu, Y. Teng, Study on the toxic interactions of Ni^{2+} with DNA using neutral red dye as a fluorescence probe, J. Lumin. 131 (2011) 705–709.
[3] L.Z. Song, X.D. Zhao, J. Fu, X.L. Wang, Y.P. Sheng, X.W. Liu, DFT investigation of Ni(II) adsorption onto MA-DTPA/PVDF chelating membrane in the presence of coexistent cations and organic acids, J. Hazard. Mater. 199–200 (2012) 433–439.
[4] G. Arthanareeswaran, P. Thanikaivelan, J.A. Raguime, M. Raajenthiren, D. Mohan, Metal ion separation and protein removal from aqueous solutions using modified cellulose acetate membranes: Role of polymeric additives, Sep. Purif. Technol. 55 (2007) 8–15.
[5] B. Kalbfuss, M. Wolff, L. Geisler, A. Tappe, R. Wickramasinghe, V. Thom, U. Reichl, Direct capture of influenza A virus from cell culture supernatant with Sartobind anion-exchange membrane adsorbers, J. Membr. Sci. 299 (2007) 251–260.
[6] K. Dermentzis, Removal of nickel from electroplating rinse waters using electrostatic shielding electrodialysis/electrodeionization, J. Hazard. Mater. 173 (2010) 647–652.
[7] R.A. Kumbasar, S. Kasap, Selective separation of nickel from cobalt in ammoniacal solutions by emulsion type liquid membranes using 8-hydroxyquinoline (8-HQ) as mobile carrier, Hydrometallurgy 95 (2009) 121–126.
[8] M.A. Barakat, E. Schmidt, Polymer-enhanced ultrafiltration process for heavy metals removal from industrial wastewater, Desalination 256 (2010) 90–93.

[9] M. Soylak, Y.E. Unsal, A. Aydin, N. Kizil, Membrane filtration of nickel(II) on cellulose acetate filters for its preconcentration, separation and flame atomic absorption spectrometric determination, Clean-Soil Air Water 38 (2010) 91–95.
[10] A.W. Mohammad, R. Othaman, N. Hilal, Potential use of nanofiltration membranes in treatment of industrial wastewater from Ni–P electroless plating, Desalination 168 (2004) 241–252.
[11] L.A. Richards, B.S. Richards, A.I. Schäfer, Renewable energy powered membrane technology: Salt and inorganic contaminant removal by nanofiltration/reverse osmosis, J. Membr. Sci. 369 (2011) 188–195.
[12] L. Lebrun, F. Vallée, B. Alexandre, Q.T. Nguyen, Preparation of chelating membranes to remove metal cations from aqueous solutions, Desalination 207 (2007) 9–23.
[13] X.D. Zhao, L.Z. Song, J. Fu, P. Tang, F. Liu, Adsorption characteristics of Ni(II) onto MA-DTPA/PVDF chelating membrane, J. Hazard. Mater. 189 (2011) 732–740.
[14] N. Flores-Holguín, A. Aguilar-Elguézabal, L.M. Rodríguez-Valdez, D. Glossman-Mitnik, Theoretical study of chemical reactivity of the main species in the α-Pinene isomerization reaction, J. Mol. Struct. Theochem. 854 (2008) 81–88.
[15] A. Srivastava, P. Rawat, P. Tandon, R.N. Singh, A computational study on conformational geometries, chemical reactivity and inhibitor property of an alkaloid bicuculline with γ-aminobutyric acid (GABA) by DFT, Comput. Theor. Chem. 993 (2012) 80–89.
[16] P. Fuentealba, J. David, D. Guerra, Density functional based reactivity parameters: Thermodynamic or kinetic concepts, J. Mol. Struct. Theochem. 943 (2010) 127–137.
[17] P. Geerlings, F.D. Proft, W. Langenaeker, Conceptual density functional theory, Chem. Rev. 103 (2003) 1793–1873.
[18] P. Pérez, A. Aizman, R. Contreras, Comparison between experimental and theoretical scales of electrophilicity based on reactivity indexes, J. Phys. Chem. A 106 (2002) 3964–3966.
[19] C.S. Zhao, X.S. Zhou, Y.L. Yue, Determination of pore size and pore size distribution on the surface of hollow-fiber filtration membranes: A review of methods, Desalination 129 (2000) 107–123.
[20] L.S. Čerović, S.K. Milonjić, M.B. Todorović, M.I. Trtanj, Y.S. Pogozhev, Y. Blagoveschenskii, E.A. Levashov, Point of zero charge of different carbides, Colloids Surf. A 297 (2007) 1–6.
[21] K. Rezaei, H. Nedjate, Diluent effect on the distribution ratio and separation factor of Ni(II) in the liquid-liquid extraction from aqueous acidic solutions using dibutyldithiophosphoric acid, Hydrometallurgy 68 (2003) 11–21.
[22] X.D. Zhao, L.Z. Song, Z.H. Zhang, R. Wang, J. Fu, Adsorption investigation of MA-DTPA chelating resin for Ni(II) and Cu (II) using experimental and DFT methods, J. Mol. Struct. 986 (2011) 68–74.
[23] R. Parthasarathi, J. Padmanabhan, V. Subramanian, B. Maiti, P. K. Chattaraj, Chemical reactivity profiles of two selected polychlorinated biphenyls, J. Phys. Chem. A 107 (2003) 10346–10352.
[24] V. Kumar, G. Jain, S. Kishor, L.M. Ramaniah, Chemical reactivity analysis of some alkylating drug molecules–A density functional theory approach, Comput. Theor. Chem. 968 (2011) 18–25.
[25] T. Boccaccio, A. Bottino, G. Capannelli, P. Piaggio, Characterization of PVDF membranes by vibrational spectroscopy, J. Membr. Sci. 210 (2002) 315–329.
[26] S.C. Zhang, J. Shen, X.P. Qiu, D.S. Weng, W.T. Zhu, ESR and vibrational spectroscopy study on poly(vinylidene fluoride) membranes with alkaline treatment, J. Power Sources 153 (2006) 234–238.
[27] A. Baraka, P.J. Hall, M.J. Heslop, Preparation and characterization of melamine-formaldehyde-DTPA chelating resin and its use as an adsorbent for heavy metals removal from wastewater, React. Funct. Polym. 67 (2007) 585–600.
[28] V.L. Silva, R. Carvalho, M.P. Freitas, C.F. Tormena, W.C. Melo, Structural determination of Zn and Cd–DTPA complexes: MS, infrared, ^{13}C NMR and theoretical investigation, Spectrochim. Acta, Part A 68 (2007) 1197–1200.
[29] G.M. Qiu, L.P. Zhu, B.K. Zhu, Y.Y. Xu, G.L. Qiu, Grafting of styene/maleic anhydride coplolymer onto PVDF membrane by supercritical carbon dioxide: Preparation, characterization and biocompatibility, J. Supercrit. Fluids 45 (2008) 374–383.
[30] H.M. Kao, C.H. Liao, A. Palani, Y.C. Liao, One-pot synthesis of ordered and stable cubic mesoporous silica SBA-1 functionalized with amino functional groups, Microporous Mesoporous Mater. 113 (2008) 212–223.
[31] M.W. McKittrick, C.W. Jones, Toward single-site functional materials–preparation of amine-functionalized surfaces exhibiting site-isolated behavior, Chem. Mater. 15 (2003) 1132–1139.
[32] S. Ek, E.I. Iiskola, L. Niinistö, Atomic layer deposition of amino-functionalized silica surfaces using N-(2-aminoethyl)-3-aminopropyltrimethoxysilane as a silylating agent, J. Phys. Chem. B 108 (2004) 9650–9655.
[33] D.D. Milenković, P.V. Dašić, V.B. Veljković, Ultrasound-assisted adsorption of copper(II) ions on hazelnut shell activated carbon, Ultrason. Sonochem. 16 (2009) 557–563.
[34] L.J. Li, F.Q. Liu, X.S. Jing, P.P. Ling, A.M. Li, Displacement mechanism of binary competitive adsorption for aqueous divalent metal ions onto a novel IDA-chelating resin: Isotherm and kinetic modeling, Water Res. 45 (2011) 1177–1188.
[35] S.S. Gupta, K.G. Bhattacharyya, Kinetics of adsorption of metal ions on inorganic materials: A review, Adv. Colloid Interface Sci. 162 (2011) 39–58.
[36] M.V. Dinu, E.S. Dragan, Heavy metals adsorption on some iminodiacetate chelating resins as a function of the adsorption parameters, React. Funct. Polym. 68 (2008) 1346–1354.
[37] B.P. Bering, M.M. Dubinin, V.V. Serpinsky, On thermodynamics of adsorption in micropores, J. Colloid Interface Sci. 38 (1972) 185–194.
[38] A. Ramesh, D.J. Lee, J.W.C. Wong, Thermodynamic parameters for adsorption equilibrium of heavy metals and dyes from wastewater with low-cost adsorbents, J. Colloid Interface Sci. 291 (2005) 588–592.
[39] D. Mohan, K.P. Singh, Single- and multi-component adsorption of cadmium and zinc using activated carbon derived from bagasse-an agricultural waste, Water Res. 36 (2002) 2304–2318.